DKF

GCA Technical Report No. 66-1-N

NASA CR 71210

PHYSICS OF PLANETARY ATMOSPHERES IV: GAS ANALYSIS BY PHOTOIONIZATION MASS SPECTROMETRY

W. Poschenrieder
P. Warneck

GCA CORPORATION
GCA TECHNOLOGY DIVISION
Bedford, Massachusetts

Contract No. NASW-1283

Prepared for

NATIONAL AERONAUTICS AND SPACE ADMINISTRATION
HEADQUARTERS
Washington, D. C.

January 1966

GAS ANALYSIS BY PHOTOIONIZATION MASS SPECTROMETRY

By W. Poschenrieder and P. Warneck

ABSTRACT

A photoionization mass spectrometer featuring a special 180-degree magnetic analyzer with inclined pole faces is described and its usefulness as a gas analytical tool is explored. The investigated range of ion source pressures was 0 to 150 microns. It was found that pressures up to 20 microns can be utilized for gas analysis. At higher pressures, ion-molecule reactions and increasing light absorption cause nonlinear ion current-pressure relationship. The major advantage of photoionization when compared to electron impact ionization is the simplicity of fragmentation patterns, the major disadvantage, the lower sensitivity. At 20 microns pressure, spark or resonance light sources used in conjunction with a 1/2-meter monochromator produced peak ion intensities around 5×10^{-13}A. Although these ion intensities are higher than those reported previously, they are still considerably below the ion intensities commonly produced by electron impact ion sources.

INTRODUCTION

Mass analysis of photoionization products has been a research subject for a number of years. The feasibility of using a photoionization source in conjunction with a mass spectrometer was first demonstrated by Lossing and Tanaka [1]* and independently by Herzog and Marmo [2], who made use of the undispersed radiation from a hydrogen or a krypton light source separated from the ion chamber by a lithium fluoride window. Addition of a monochromator for photon energy selection by Professor Inghram's group [3-5] greatly increased the versatility of this method, although the use of a lithium fluoride window still restricted the accessible energy range to less than 11 eV. This barrier was overcome with the application of differential pumping techniques together with advances made in developing suitable vacuum ultraviolet light sources. Weissler, et al. [6], Schönheit [7,8], Comes, et al. [9,10] and Schoen [11] all employed low pressure spark sources which provide a spectrum rich in lines. Dibeler and collaborators [12-14], in contrast, recently have used high pressure argon and helium continuous light sources. The increasing sophistication of instrumentation has brought forth much needed data including ionization onsets, ionization efficiencies, fragmentation ratios, and kinetics of ion formation, but it appears that the potentialities of the photoionization mass spectrometer as a gas analyzer have not been exploited. This possibility will be explored in the present paper. Analytical application is an aspect worth consideration because it offers several advantages over the conventional electron impact technique.

*Numbers in [ ] throughout text represent reference numbers.

One overriding feature that became apparent in the early investigations is the simplicity of fragmentation patterns. Often, the parent peak is the sole contributor to the mass spectrum. In contrast, the analysis of electron impact mass spectra of even simple gas mixtures is made difficult because of the complexity of fragmentation patterns. It is true that fragmentation can be minimized if an electron impact source is operated at low electron energies, but the resulting loss in sensitivity can usually not be tolerated. The ease of photon energy selection and the higher photoionization cross sections near threshold when compared to the corresponding electron impact parameters constitute additional advantages. Other benefits derive from the absence of a hot filament otherwise necessary to produce electron emission: (a) the ion source can be kept at room temperature, and (b) any perturbing chemical interactions between sample gas and the heated filament are ruled out.

The major drawback of the photoionization mass spectrometer when compared with electron impact type instruments is its lower sensitivity. The lower sensitivity stems from the fact that to date copious amounts of electrons are generated more easily than high photon fluxes. It, however, can be shown that instrumental factors must also be considered. Hurzeler, et al. [3] quote maximum ion currents of 10^{-15} A, Dibeler and Reese [12] obtained only 10^{-17} A. If these were the optimum achievable ion currents, the prospects of utilizing the photoionization mass spectrometer for sensitive gas analysis would be indeed dim. Fortunately, the situation can be improved.

To date, light intensities of the order of 10^9 photons/sec can be attained at the exit slit of a monochromator provided strong emission lines are selected. If 10 percent of this intensity could be utilized for ion production, with an ionization efficiency of about 50 percent, and if further an ion collection efficiency of 10 percent is assumed, the resulting ion current is 8×10^{-13} A or more than one hundred times higher than that quoted by Hurzeler, et al. [3]. However, this estimated improvement can be realized only with ion source pressures high enough to insure the absorption of an appreciable fraction of the available light intensity; in addition, the ion collection efficiency must be favorable. Most of the previous investigators worked with ion source pressures in the 10^{-4} mm Hg range corresponding to less than one tenth of a percent light absorption. They mostly used analyzers of the 60 degree sector field type which are characterized by a small solid angle collection efficiency and a correspondingly low factor of transmission. Comes and Lessman [9] employed a quadrupole mass analyzer but similarly were forced to work with wide apertures at the expense of resolution to obtain desirable ion intensities.

In view of the possibilities for improvement, the main interest of the present work was to explore the usefulness of a photoionization mass spectrometer operating at ion source pressures in the 10 to 100 micron range; to adapt a special 180 degree magnetic analyzer with wide solid angle ion acceptance for this purpose; and to determine the characteristics of this instrument with respect to its gas analytical applicability. A detailed description of the apparatus and its performance is presented in the following sections.

APPARATUS

Except for the modifications already noted, the apparatus employed known principles. Thus, the apparatus incorporated a discharge light source, a vacuum ultraviolet grating monochromator, the ion source, a photon detector, a 180-degree magnetic analyzer with electron multiplier detector, and associated electronics. The integrated experimental arrangement is shown in Figure 1.

A. Light Source and Monochromator

Two types of light sources were employed; one, a dc cold cathode discharge lamp based on a design by Hunter [15] which emits a continuous flux of photons from a plasma maintained in an uncooled quartz capillary. With hydrogen as the excited gas, the emission consists of a many line spectrum useful at wavelengths above 850Å. In rare gases, mainly the resonance lines are emitted, vis. HeI 584Å, NeI 735Å, NeI 745Å, AI 1048Å, AI 1066Å. The second type of light source was a repetitively pulsed spark discharge using a ceramic capillary. This source is similar to that described by Weissler, et al. [6]. It emits a spectrum of widely spaced lines mainly in the region 400 to 1000Å with maximum intensities comparable to those of the rare gas lines.

The monochromator was a McPherson 1/2-meter Seya instrument, fitted with a 1200 lines/mm tripartite replica grating blazed for 750Å. The head bearing the exit slit assembly was removed from the exit arm of the monochromator and replaced by a tubular section accommodating the mass spectrometer ion source. The optical entrance slit of the ion source served as the new monochromator exit slit. With the slit jaws set to a width of 250 microns, the observed wavelength resolution was approximately 5Å. At 750Å, this corresponds to an energy resolution of 0.1 eV.

B. Ion Source

The arrangement of the ion source is shown in Figure 2. The light entrance slit is preceded by a wider slit which baffles the light beam and maintains a pressure differential between the ion source housing and the monochromator. Appropriately biased, this slit also collects any photoelectrons formed at the ion source entrance slit. The light beam leaves the ion source through a slot again sufficiently wide to prevent the formation of photoelectrons from photons striking the walls. The slot is used at this point rather than a slit because it reduces the gas flow out of the ion source and minimizes penetration of the field set up between the ion source and the housing. After the light beam passes through the ion source, it falls upon a sodium salicylate-coated glass plate viewed by a photomultiplier. Dibeler and Reese [12] stated that the quantum yield of the coating if affected by exposure to hydrocarbon vapors. No such effect has been observed in the present work. Although the photoelectric detector used by Dibeler and Reese [12] allows the determination of absolute photon fluxes, preference has been given here to the sodium salicylate

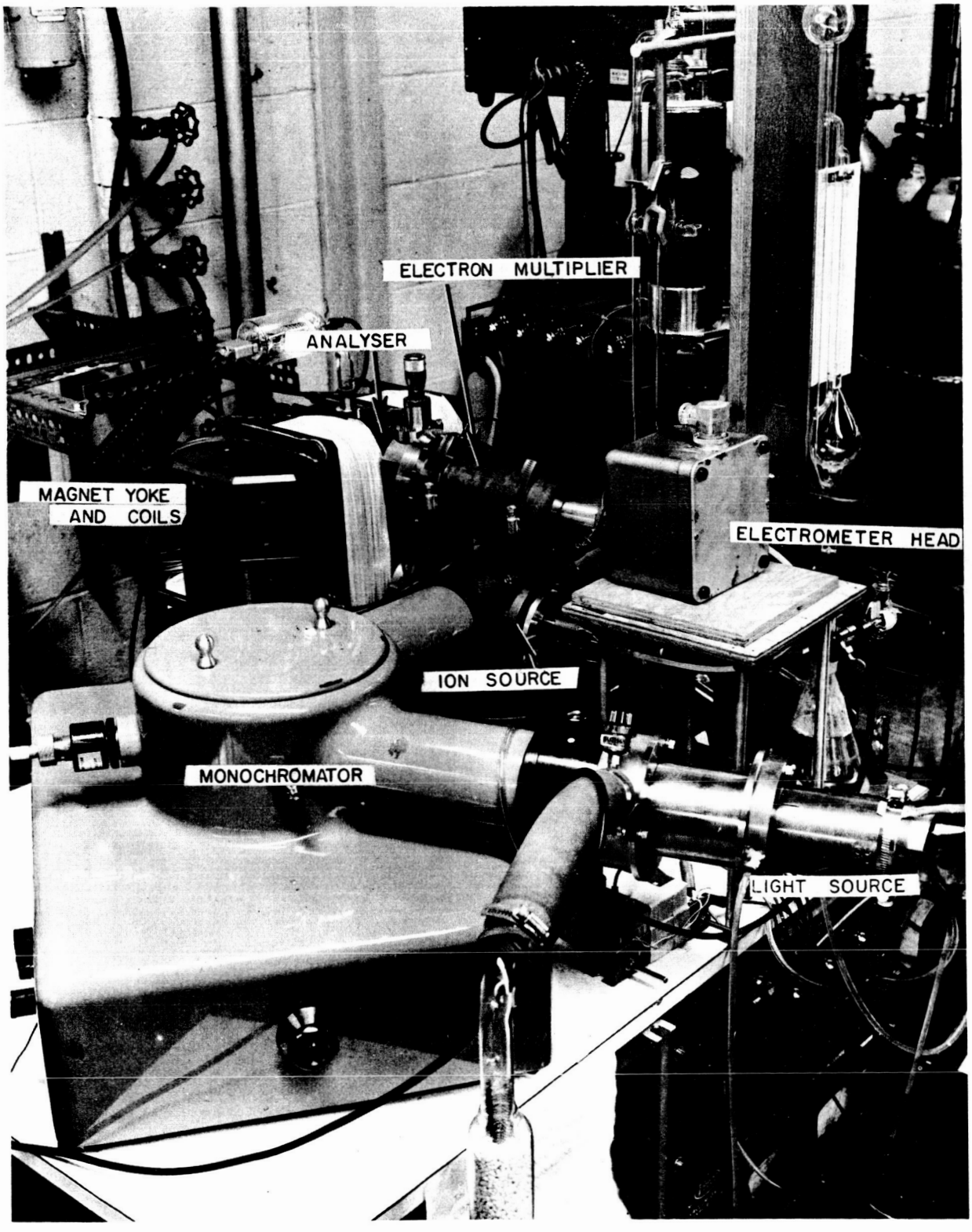

Figure 1. Photoionization mass spectrometer.

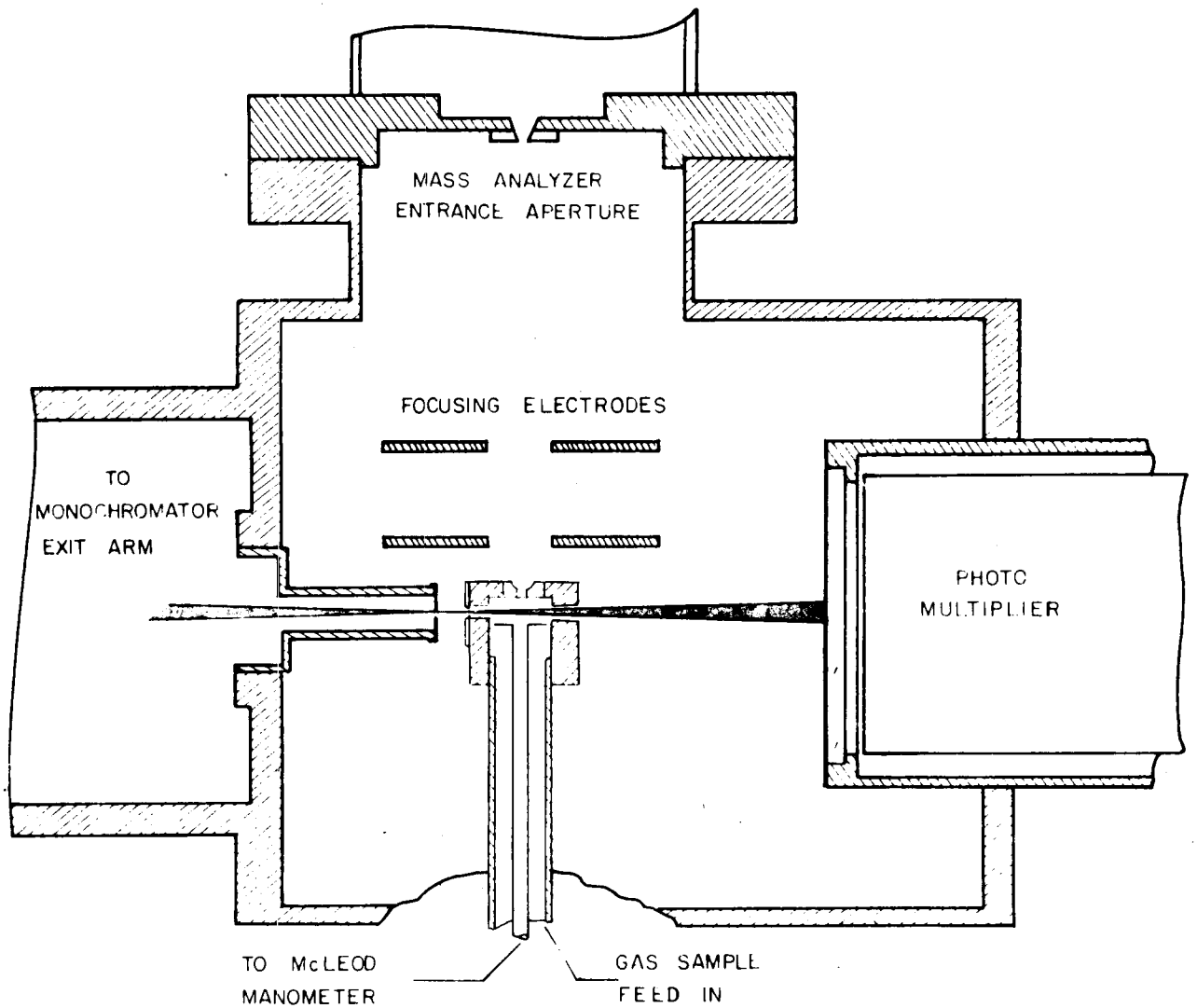

Figure 2. Schematic of ion source.

converter because its quantum yield is approximately constant over a wide wavelength region [16]. Intensity comparisons are thereby facilitated.

Owing to the stigmatic focussing properties of the mass analyzer, the ion source geometry has been made cylindrical, coaxial with the center of the ion beam. Photoions are removed from the ionization region in the conventional manner with the use of a positively-charged repeller plate. The repeller, brought into position several millimeters away from the light beam by a micrometer screw, is attached to a steel tube through which the gas pressure in the ion source can be measured directly with a McLeod gauge. An insert opposite the repeller allows for a change in size of the ion extraction orifice. Ions are accelerated and focussed onto the analyzer entrance by an immersion lens system consisting of two plates with 1/2-inch openings. Each plate divided into halves permits ion beam adjustment in the vertical and horizontal directions. The second plate is charged slightly negatively with respect to ground potential so that secondary electrons conceivably formed by interaction of the ion beam with the analyzer entrance aperture are prevented from being accelerated back into the ion source.

C. Mass Analyzer and Detector

The particular need of the photoionization product analyzer to provide good ion transmission characteristics called for an analyzer with wide solid-angle focussing properties. The present apparatus, therefore, uses a 180 degree magnetic analyzer with inclined pole faces. A similar device was previously applied as a β-spectrometer but apparently not in conjunction with mass spectrometers. The basic theory is well established [17] and it has been shown that for a special selected ion orbit, fully stigmatic focussing occurs with the image aberration in the center plane vanishing up to the fourth order [17,18].

In the present design, entrance and exit apertures are six inches apart so that the spectrometer may be compared to a conventional 180 degree analyzer of three inches radius. However, because of the wedge-shaped air gap, the ions move on cycloidal orbits rather than circular ones. Entrance and exit apertures are located outside the magnetic field on the line where both planes of the pole faces intersect. The distance from the magnetic field boundary is given by the theory as 2.185 inches for the chosen distance of six inches between the apertures. The angle of inclincation between the two pole faces is 11 degrees. The actual aperture has been made smaller (10 degrees) so that ions would not strike the pole pieces. Herzog [19] shunts control the magnetic fringe field. The theoretical mass resolution of this device is calculated for 1 mm entrance and exit orifices as $M/\Delta M = 65$, the half width resolution being 130. The resolution of a conventional spectrometer of comparable dimensions is only 35 and the available aperture at best 1 degree. This clearly indicates the superiority of the present design.

Mechanically, the analyzer consists of a box 2.5 x 3.5 x 7.5 inches, welded together from stainless steel plates and integrated with the wedge-

shaped pole pieces. An electromagnet with symmetrical coil arrangement adjacent to the chamber provides a maximum magnetic induction of about 4000 gauss in the center portion of the analyzer gap. The rather heavy magnet plus the analyzer are mounted on a precisely guided carriage. This facilitates focussing adjustments. Connection to the ion source housing is via stainless steel bellows. The exit slit assembly incorporates the usual suppressor arrangement as well as deflection electrodes to focus the ion beam onto the first dynode of a 20-stage electron multiplier. The inactivated magnesium-doped aluminum dynodes are insensitive to atmospheric pressure. Maximum amplification of about 10^6 was achieved but a gain of 10^4 usually was sufficient. Magnetic shielding avoids loss of gain by stray magnetic fields at higher magnet currents. The electron multiplier output current is fed to a vibrating reed electrometer via a 10^{11} ohm input resistance. Auxiliary ion collectors are provided behind the analyzer entrance and its exit orifice for independent ion beam observation.

D. Pump Arrangement

The key to a successful operation of the integrated apparatus is the application of differential pumping. Light source pressures are in the 100 micron range, while the monochromator chamber should be kept at pressures below 10^{-4} torr mainly so that intensity losses from optical absorption are avoided. Similarly, it is desirable to operate the ion source at pressures in the 10 to 100 micron region, whereas in the mass analyzer chamber, pressures much above 10^{-5} torr cannot be tolerated because of ion beam scattering. These requirements are met by the following pumping stages: The monochromator is evacuated with a nominal 4-inch oil diffusion pump of 700 liter/sec rated speed, but this rate is scaled down by a factor of two owing to the use of a freon refrigerated baffle. The light source is differentially pumped with a 375 liter/min mechanical pump. The gas escaping the ion sources is taken up by another 4-inch oil diffusion pump to reduce the pressure in the ion source by a factor of about one hundred. The mass analyzer, finally, is evacuated by a 2-inch oil pump likewise fitted with a freon-cooled baffle. All diffusion pumps are backed up by a single 375 liter/min mechanical pump. As an example of the efficiency of the described arrangement, pressures observed with an ion source pressure of 50 microns are: light source pump line 200 microns; monochromator 5×10^{-5} torr; ion source housing 2×10^{-4} torr; mass analyzer chamber 2×10^{-6} torr.

PERFORMANCE

The instrument has been evaluated with respect to mass resolution, ion current-pressure relationship, fragmentation patterns, and overall sensitivity. In addition, an examination has been made of the possibility to discriminate mass doublets by their difference in ionization onsets.

A. Analyzer

The achieved effective mass resolution was determined for krypton which was ionized by the group O III spark discharge lines around 835Å which corresponds to 0.8 eV above the ionization threshold. Figure 3 shows a trace of the ion current obtained when the magnetic field was scanned. The five stable isotypes of krypton in the e/m-78 to 86 mass range are all displayed. The peaks at mass numbers 82 and 83 are well separated, indicating a resolution of $m/\Delta m = 82$ with a 15 percent valley. The average resolution determined from the half width of the peaks is $m/\Delta m = 125$, in surprisingly good agreement with the expected resolution since no particular effort was made to achieve optimum ion beam adjustment.

While the krypton mass spectrum was obtained with ion source pressures around 20 microns, it was observed that most of the stronger peaks in any mass spectrum broadened and developed tails to the lower energy side at pressures exceeding 20 microns. The tails could be cut off by the suppressor. Up to 100 microns pressure, the situation could also be improved if the ion source exit aperture was reduced. This shows that the asymmetry of the peaks is caused by ion-neutral collisions in the acceleration region outside the ion source. From the integrated peak intensities, it could be inferred that the predominant portion of the scattered ions were collected into the analyzer. Clearly, this is due to the wide solid angle collection efficiency of the analyzer.

B. Pressure Dependence

The present study of photoionization differs from previous investigations in that ion source pressures were in the 10 to 100 micron region, whereas previous experimenters employed ion source pressures in the 10^{-4} mm Hg range. The higher pressures result in an increase in photon absorption and correspondingly higher ion intensities. Obviously, the pressures cannot be increased indefinitely due to nonuniform light absorption on one hand and interference of ion molecule reactions on the other.

The ion current emerging from the ion source exit aperture is $i = Ae\gamma I [1 - \exp(-\sigma nL)]$. Here, e is the charge of the electron, I the effective light intensity, γ the ionization efficiency, and σ the absorption cross section of the gas at the wavelength considered, n the gas number density, and L the length of the effective ionization region. A is a factor taking into

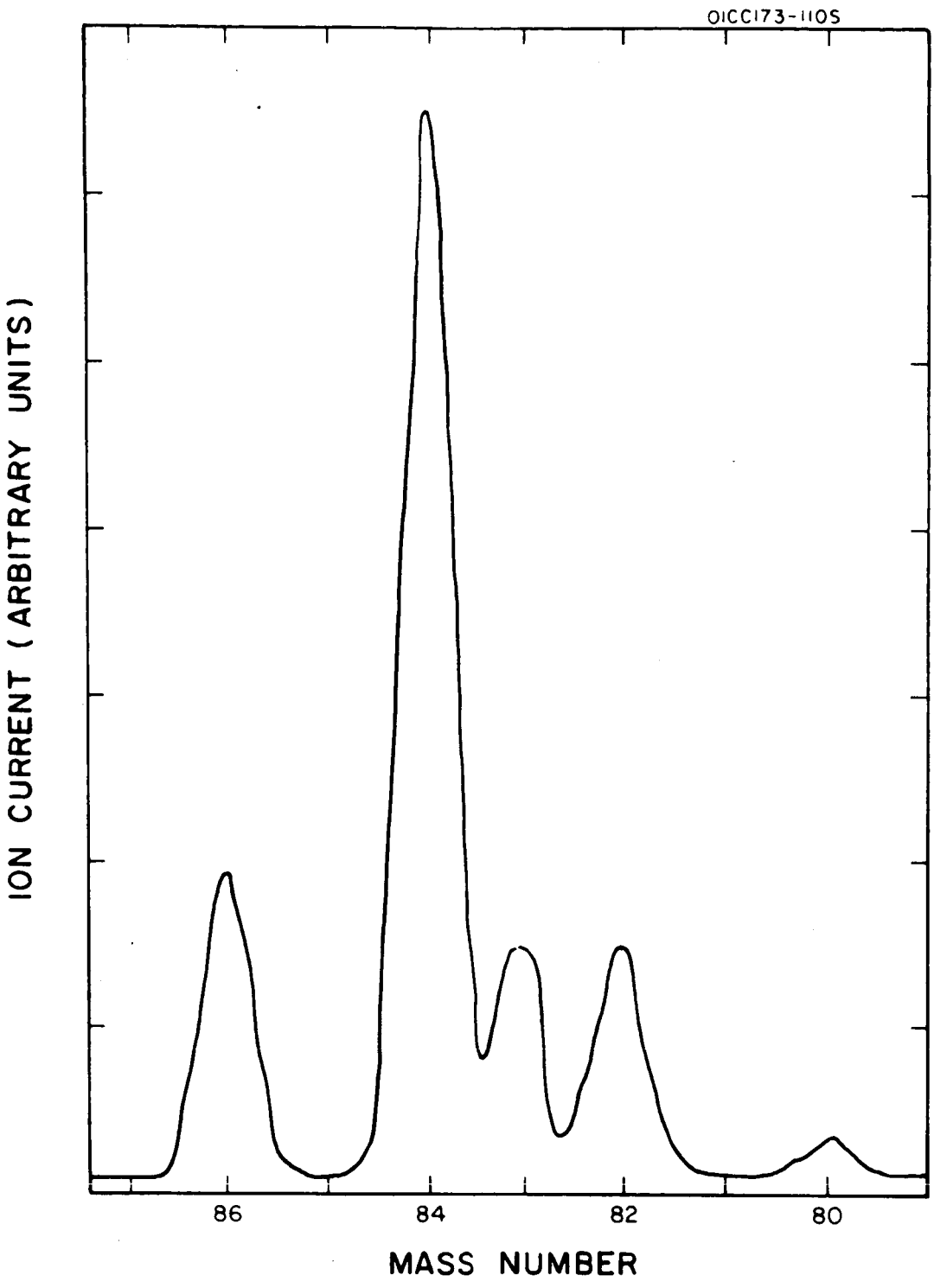

Figure 3. Magnetically scanned krypton spectrum. Ionizing wavelength 835Å.

account that the efficiency for ion collection is not unity. So long as optical absorption in the ion source is negligible, the effective light intensity is equal to the incident light intensity I_o, and by expansion of the exponential function, the ion current becomes $i = AeI_o\gamma\sigma nL$ in first approximation, i.e., the ion current observed is proportional to the pressure. At high pressures, increasing absorption renders this approximation invalid. In addition, nonlinearity can be caused by insufficient spectral resolution in a wavelength region where absorption cross sections, or ionization efficiencies, or both strongly vary with wavelength. The influence of these effects is clearly displayed in Figure 4 which shows N_2^+ and O_2^+ ion currents generated at 584Å wavelength as a function of pressure. For O_2^+, linearity persists up to 150 microns but N_2^+ displays nonlinearities due to light absorption at pressures greater than 60 microns so that the useful pressure range is limited.

The influence of ion-molecule reactions is more severe. It became particularly noticeable when hydrogen or organic gases were admitted to the mass spectrometer. Figure 5 demonstrates this situation for methane, with two different repeller voltages being employed to indicate the increasing influence of the reaction $CH_4^+ + CH_4 \rightarrow CH_5^+ + CH_3^+$ at lower repeller fields. This is due to an increase of ion residence times in the ion source. According to the theory of ion molecule reactions in a mass spectrometer ion source [20], the residence time is $t = (2dm/eE)^{1/2}$, where d is the distance from the light beam to the ion exit aperture, m is the mass of the primary ion, e is the charge of the electron, and E is the applied electric field. The data shown in Figure 5 were obtained with d = 0.3 cm, so that $t = 3.1 \times 10^{-6}$ sec for 1 volt repeller voltage and $t = 1.6 \times 10^{-6}$ sec for 10 volt repeller voltage. From these data, the rate constant for the methane reaction can be calculated as $k = 1.3 \times 10^{-9}$ cc/molecule sec, respectively, $k = 1.0 \times 10^{-9}$ cc/molecule sec, in good agreement with the results obtained by Martin and Melton [21], and by Field, et al. [22]. In the high pressure regime, therefore, the instrument is ideally suited to studies of ion-molecule reactions. Some results of such studies have already been reported [23].

In the present application, the occurrence of ion-molecule reactions is an undesirable side effect. Although the conversion of one type of ion to another occurring at a different mass number can at times be beneficial to mass analysis, it hampers the attempt to simplify the mass spectrum by photoionization and it introduces nonlinearities in the ion-current pressure relationship. It was, however, anticipated that ion molecule reactions could be suppressed by lowering the ion residence time appropriately. Indeed, ion residence times as low as $t = 0.2 \times 10^{-6}$ sec were achieved by making $d \leq 0.1$ cm and $E \geq 15$ volt/cm. Under these conditions, the parent ion currents in hydrogen, methane, etc. were linear up to 20 microns ion source pressure, and the intensity of the daughter ion was less than 5 percent of the parent ion intensity. Improved suppression of ion-molecule reactions was observed at lower pressures. However, it is clear that the occurrence of ion molecule reactions further restricts the useable pressure range, and that, at present, a pressure of 20 microns constitutes the upper limit to the region where ion currents follow an essentially linear pressure dependence.

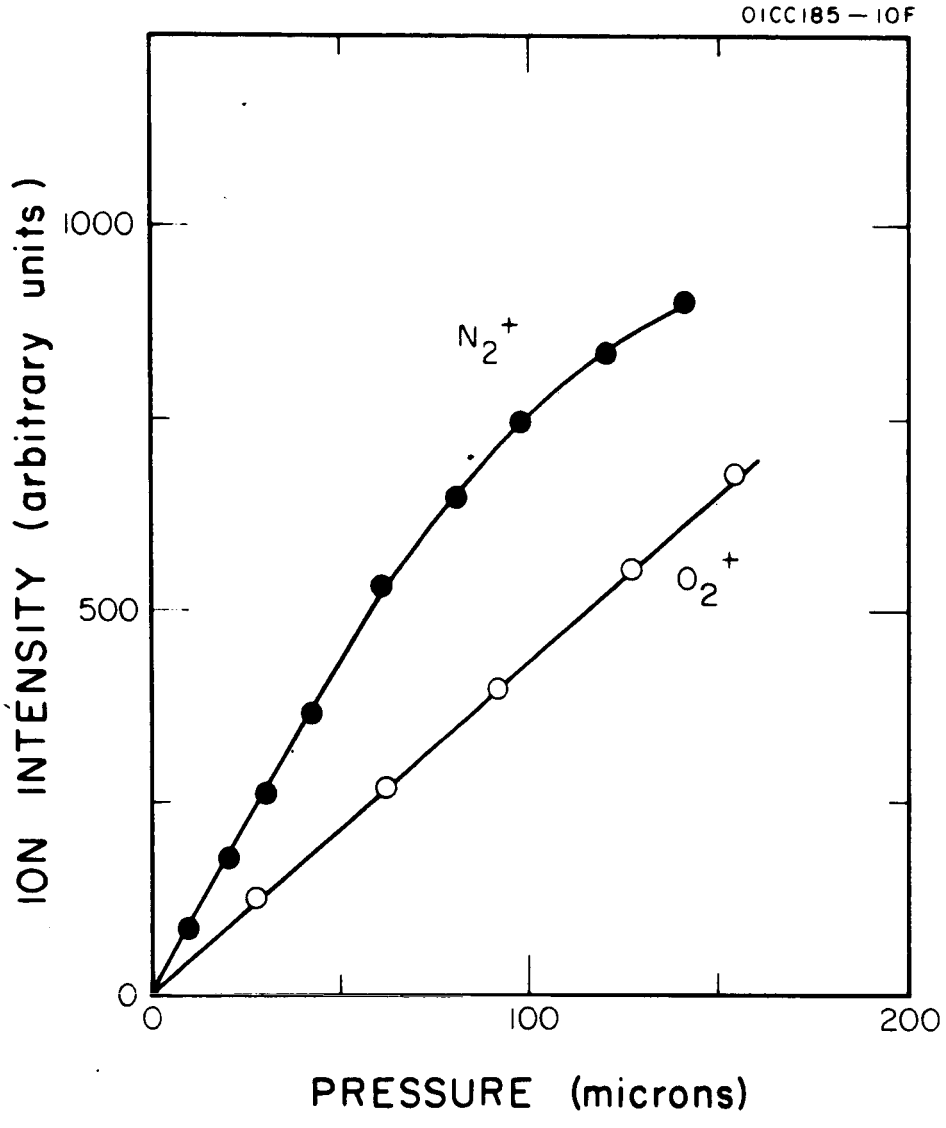

Figure 4. Ion intensity - pressure relationship for nitrogen and oxygen ionized at the wavelength of the helium resonance line at 584Å.

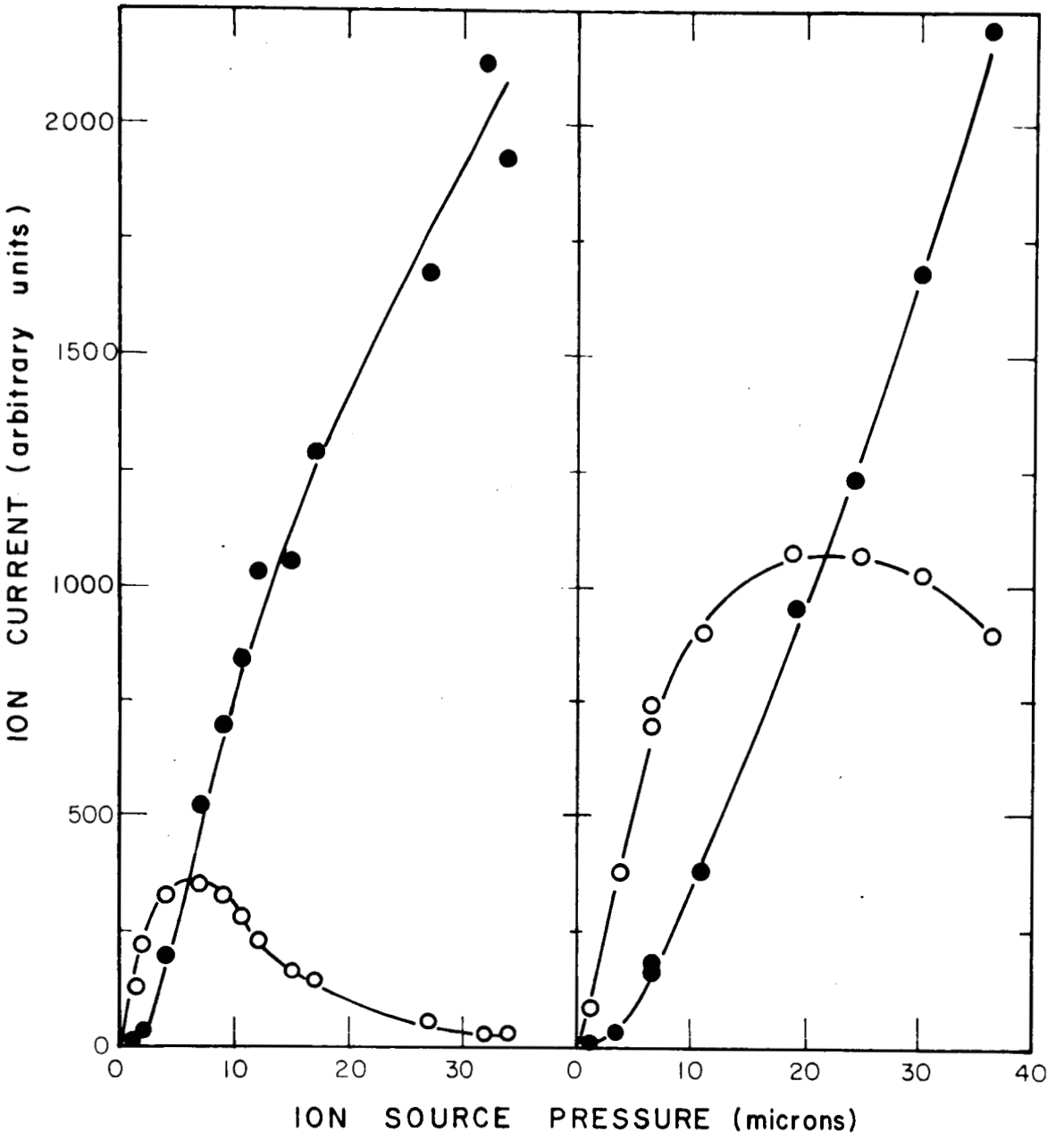

Figure 5. Ion-molecule reaction in methane ionized at 922Å wavelength. Left: 1 volt repeller; right: 10 volt repeller. Open circles refer to mass 16 ions, closed circles to mass 17 ions.

C. Sensitivity

Generally, the ion currents observed at the mass spectrometer collector were of the expected order of magnitude. However, owing to the pressure effects discussed above, it was not practical to operate in the pressure range where the degree of light absorption reaches 10 percent. At pressures around 10 microns, the extent of light absorption is approximately 1 percent so that the expected ion intensity outside the source is 8×10^{-14} A. Maximum observed ion currents were about 5×10^{-13} A at pressures around 20 microns in accordance with expectation, and routinely observed parent peak intensities averaged 1×10^{-13} A. At the lower end of the scale, ion currents of the order of 10^{-19} A could be detected but the accompanying fluctuations were excessive with the employed detector response speed of 0.5 seconds. Better signal integration is definitely required in this low current range. Ion currents around 10^{-17} A could be recorded with reasonable accuracy. The practical operating range of the present arrangement, therefore, is 1×10^{-17} - 1×10^{-13} A with a signal noise level around 0.5×10^{-17} A. For comparison, we note the specifications for a CEC 21-611 mass spectrometer available in this laboratory. This instrument features a current range between 5×10^{-14} and 1×10^{-10} A at the ion collector, with an empirical noise level of perhaps 5×10^{-15} A in the lower current region. The CED mass spectrometer operates with 20μA electron current corresponding to a flux of 1.2×10^{14} electrons/sec, compared to the above 10^{9} photons/sec light intensity used for photoionization.

Relative sensitivities for various gases were determined at the wavelengths of the helium and neon resonance lines, in conjunction with fragmentation data to be reported below. Nitrogen was used as a reference gas. The results shown in Table 1 together with similar data obtained for the CEC instrument provide a comparison with electron impact sensitivities. Rather uniform relative sensitivities are observed at 584Å and with the CEC mass spectrometer. The sensitivity for hydrogen is below average in both cases. Greater variation in the sensitivities is observed at the near resonance lines at 735.9Å and 743.7Å where absorption cross sections and photoionization efficiencies vary sharply for many gases. The 735.9Å is more intense and also the sensitivity variations are less pronounced than at 743.7Å so that this line is preferable for gas analysis when a neon light source is employed.

Photoionization at the wavelengths of the helium and neon resonance lines has been investigated mainly because of the favorable intensity of these lines and because they are nearly isolated features in the photoionization region. This permits operation of the monochromator with wide optical slits so that the available light intensities may be fully utilized. Data concerning the degree of fragmentation at these resonance lines are given below.

D. Fragmentation

As pointed out earlier, the outstanding virtue of the photoionization mass spectrometer is that it minimizes the contribution of fragment ions to the observed mass spectrum. Of course, minimum fragmentation products are

TABLE 1

RELATIVE SENSITIVITIES FOR VARIOUS GASES

	He 584Å	Ne 735.9Å	Ne 743.7Å	CEC MS
N_2	1.0	1.0	1.0	1.0
A	1.45	1.6	1.35	0.96
O_2	0.97	2.1	0.76	0.70
CO	1.0	1.4	0.86	1.03
CO_2	1.31	1.3	0.69	0.903
H_2	0.665	*	*	0.57
CH_4	1.57	1.8	1.4	1.33
C_2H_4	1.10	2.2	1.65	1.09
C_2H_2	0.79	2.5	2.0	1.55

*Not measured

obtained near the threshold of ionization for any particular sample gas, but even at 25 eV photon energy, the degree of fragmentation is tolerable when compared to that observed for electron impact. Fragmentation data at the resonance lines of neon at wavelengths of 735.9Å and 743.7Å and of helium at 584Å are assembled in Table 2. Similar data obtained with the CEC 21-611 mass spectrometer are also entered in Table 3 to provide comparison between fragmentation due to photoionization and impact by 70 eV electrons.

Among the gases investigated, no fragmentation is observed at the wavelengths of the neon resonance lines, as expected, notable exceptions being methane and ethylene. Acetylene apparently does not give fragment ions. At 584Å, most gases produce fragment ions. Among the diatomic molecules, oxygen yields the highest fragment ion intensity (about 20 percent) but higher ion intensities are observed for the hydrocarbons. In most cases, it is found that electron impact results in a much higher degree of fragmentation than photon impact. For example, ethylene when subjected to electron impact yields ten different types of ions, whereas photoionization results in only four, even at the high energy provided by the helium resonance line. However, heavier hydrocarbons having lower ionization potentials undoubtedly show a considerably degree of fragmentation at these higher photon energies as can be inferred from the work of Inghram and collaborators [3-5] at photon energies below 11 eV. The photoionization fragmentation ratios shown in Table 2 are in good agreement with previous measurements available. For example, similar relative fragment ion intensities have been observed for methane by Dibeler, et al. [14], and for O_2, CO, CO_2 at 584Å by Weissler, et al. [6].

Isotopic abundances were determined in several cases. Most of the abundances found were larger than the known natural abundance entered in the last column of Table 2, but precision measurements were not within the scope of the present work. Nevertheless, order-of-magnitude values are in good agreement with the natural abundance figures. It is noted that most of the abundance values are too large rather than too small. This probably indicates a systematic error owing to neglect of signal background, etc. Indeed, the larger ^{13}C abundance is in better agreement with the established value than the smaller ^{18}O or ^{15}N abundances. This trend becomes more evident when the results obtained for krypton are considered. In this case, the natural abundance ratios are more favorable for measurement (see Figure 3) and they can be determined rather precisely as Table 3 attests.

Table 4 illustrates the relative intensity distribution in a mass spectrum of a mixture, with air as the chosen sample. For comparison, the relative photoionization product ion distribution was also calculated from the photoionization cross sections shown in the fifth column [26], and the known relative concentrations of nitrogen, oxygen, argon, and carbon dioxide in air of standard composition. The results are in good agreement, only CO_2 shows a stronger concentration in the measured sample indicating an excess of carbon dioxide.

TABLE 2

FRAGMENTATION AND ISOTOPE ABUNDANCE RATIOS FOR VARIOUS GASES.
COMPARISON OF PHOTOIONIZATION AND ELECTRON IMPACT DATA.

Sample Gas	e/m	Assignment	He 584Å	Ne 735.9Å	Ne 743.7Å	CEC MS	Natural Abundance
N_2	29	$^{14}N^{15}N^+$	0.0080	*	*		0.00367
	28	$^{14}N_2^+$	1.0	1.0	1.0	1.0	1.000
	14	N^+, (N_2^{++})	---	---	---	0.084	----
A	40	$^{40}A^+$	1.0	1.0	1.0	1.0	1.000
	38	$^{38}A^+$	0.0013	0.0009	*	*	0.00062
	36	$^{36}A^+$	0.0039	0.0044	0.0052	0.0039	0.00338
	20	A^{++}	---	---	---	0.340	----
O_2	34	$^{18}O^{16}O^+$	0.0041	0.0039	0.0059	*	0.00204
	33	$^{17}O^{16}O^+$	*	0.0013	*	*	0.00037
	32	$^{16}O_2^+$	1.0	1.0	1.0	1.0	1.000
	16	O^+, (O_2^{++})	0.21	---	---	0.064	----
CO	30	$^{12}C^{18}O^+$	0.0015	0.0024	0.0036	*	0.00205
	29	$^{13}C^{16}O^+$	0.012	0.0113	0.0162	*	0.0112

TABLE 2 (continued)

Sample Gas	e/m	Assignment	He 584Å	Ne 735.9Å	Ne 743.7Å	CEC MS	Natural Abundance
CO	28	$^{12}C^{16}O^{+}$	1.0	1.0	1.0	1.0	1.000
	16	O^{+}	---	---	---	0.0017	----
	14	CO^{++}	---	---	---	0.014	----
	12	C^{+}	0.0037	---	---	0.014	----
CO_2	46	$^{12}C^{18}O^{16}O^{+}$	0.0038	0.006	*	*	0.0204
	45	$^{13}C^{16}O_2^{+}$	0.0113	0.0125	0.0136	*	0.0112
	44	$^{12}C^{16}O_2^{+}$	1.0	1.0	1.0	1.0	1.000
	28	CO^{+}	0.0151	---	---	0.0662	----
	22	CO_2^{++}	---	---	---	0.0432	----
	16	O^{+}	0.054	---	---	0.113	----
	12	C^{+}	---	---	---	0.0416	----
H_2	2	H_2^{+}	1.0	1.0	1.0	1.0	----
	1	H^{+}	0.020	---	---	*	----

TABLE 2 (continued)

Sample Gas	e/m	Assignment	He 584Å	Ne 735.9Å	Ne 743.7Å	CEC MS	Natural Abundance
CH_4	17	$^{13}CH_4^+$	*	*	*	0.0123	0.0112
	16	$^{12}CH_4^+$	1.0	1.0	1.0	1.0	1.000
	15	CH_3^+	0.975	0.94	0.825	0.079	----
	14	CH_2^+	0.0325	0.0355	0.0325	0.086	----
	13	CH^+	---	---	---	0.038	----
	12	C^+	---	---	---	0.0147	----
C_2H_4	28	$C_2H_4^+$	1.0	1.0	1.0	1.0	----
	27	$C_2H_3^+$	0.86	0.79	0.79	0.572	----
	26	$C_2H_2^+$	0.40	0.39	0.373	0.525	----
	25	C_2H^+	---	---	---	0.074	----
	24	C_2^+	---	---	---	0.025	----
	16	CH_4^+	---	---	---	0.0109	----
	15	CH_3^+	---	---	---	0.0098	----
	14	CH_2^+	0.0175	---	---	0.0362	----

TABLE 2 (continued)

Sample Gas	e/m	Assignment	He 584Å	Ne 735.9Å	Ne 743.7Å	CEC MS	Natural Abundance
C_2H_4	13	CH^+	---	---	---	0.0163	----
	12	C^+	---	---	---	0.0109	----
C_2H_2	26	$C_2H_2^+$	1.0	1.0	1.0	1.0	----
	25	C_2H^+	0.20	---	---	0.197	----
	24	C_2^+	0.004	---	---	0.0525	----
	15	CH_3^+	0.0053	---	---	0.0033	----
	14	CH_2^+	---	---	---	0.0031	----
	13	CH^+	0.002	---	---	0.0742	----
	12	C^+	---	---	---	0.0145	----

*Not measured

TABLE 3

RELATIVE INTENSITIES OF THE KRYPTON ISOTOPES OBSERVED

e/m	Intensities Observed	Natural Abundances
80	0.039	0.040
82	0.201	0.203
83	0.201	0.203
84	1.000	1.000
86	0.293	0.305

TABLE 4

ION INTENSITIES IN AIR

e/m	Assignment	Ion Intensity	Relative Ion Intensity	σ_i Mb	Relative Photoion Production
16	O^+	78	0.037	3.8	0.034
18	H_2O^+	58	0.003	----	-----
28	$^{14}N_2^+$	1620	0.775	23.1	0.780
29	$^{14}N^{15}N^+$	8	0.004	----	-----
32	O_2^+	370	0.177	18.9	0.171
40	A^+	26	0.013	36.5	0.0146
44	CO_2^+	45	0.002	33.9	0.0006

E. Discrimination of Mass Doublets

The convenience with which good photoionizing energy resolution can be obtained with a monochromator of only moderate wavelength resolution may be utilized to discriminate between gas samples yielding similar or overlapping mass spectra. Table 5 illustrates this point for several well known mass doublets. All pairs have ionization potentials sufficiently far apart to allow discrimination of ionization onsets by an appropriate choice of wavelength setting. For example, photons in the 889Å to 961Å wavelength region interacting with a N_2O-CO_2 gas mixture ionize N_2O but not CO_2. Similarly, one can ionize CO in the presence of N_2 in the 796Å to 885Å wavelength region without simultaneously ionizing N_2. Figure 6 shows the trace of ion currents obtained in nitrogen and carbon monoxide in the wavelength region of interest. The spark light source fed with argon was used in this experiment. The variation of light intensity recorded by the photomultiplier is shown at the bottom of Figure 6. The separation of ionization onsets is clearly displayed, but experimental difficulties inherent in the suggested procedure are also made apparent. As indicated in Figure 6, the ion current of both CO^+ and N_2^+ is not exactly nil at wavelengths above the ionization threshold. At these wavelengths, ionization is due to second order spectral interference and possibly scattering of short wavelength radiation. Separation of mass doublets by wavelength discrimination, therefore, is still an imperfect procedure [24].

TABLE 5

IONIZATION THRESHOLDS FOR SEVERAL MASS DOUBLETS

Doublet	e/m	Ionization Potential eV	Wavelength Å
CO_2	44	13.79	889
N_2O		12.90	961
NO	30	9.25	1340
C_2H_6		11.65	1064
N_2	28	15.58	796
CO		14.01	885
C_2H_4		10.51	1179
C_2H_2	26	11.41	1086
CN		15.13	819

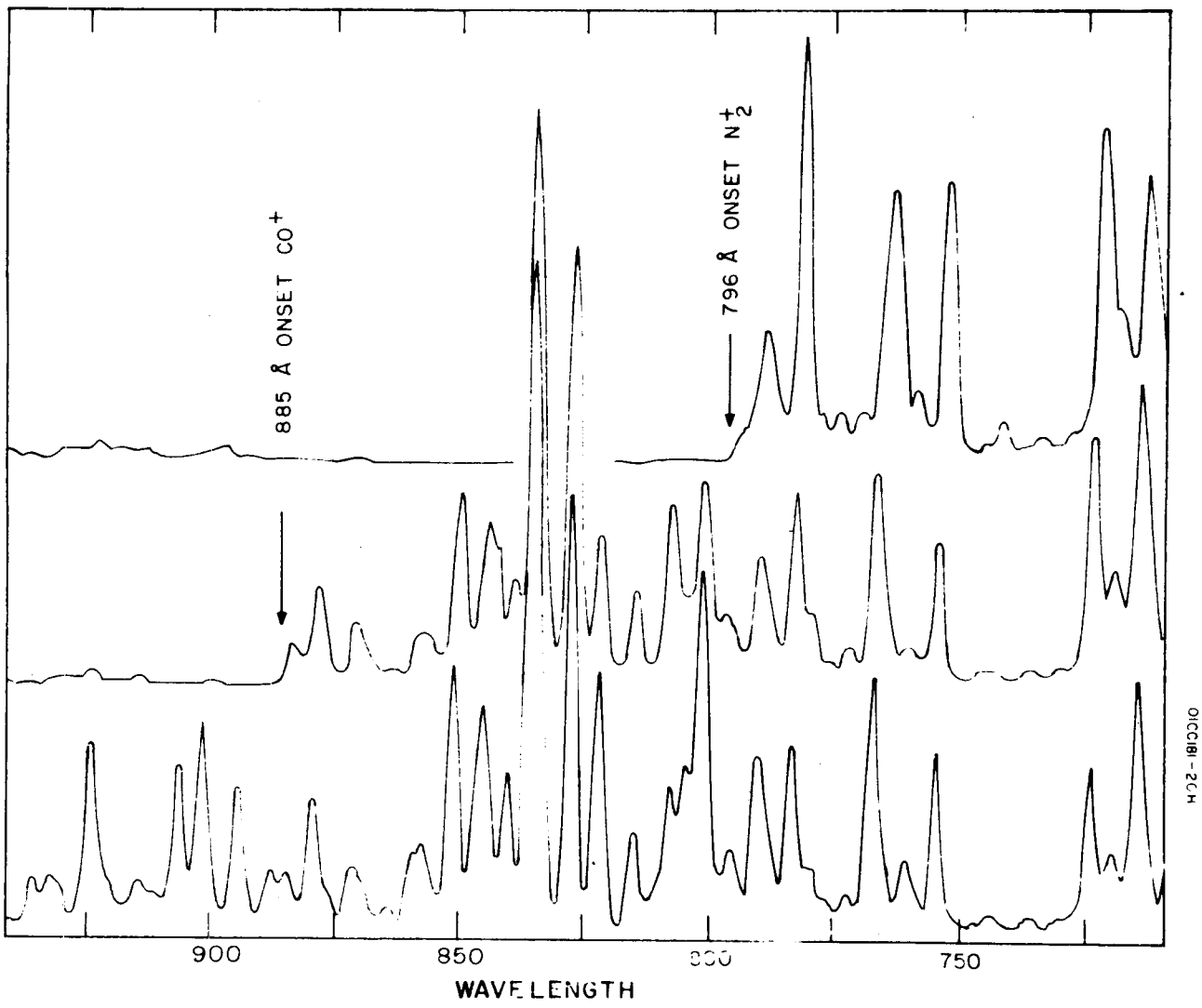

Figure 6. Comparison of nitrogen and carbon monoxide ionization as a function of wavelength. Upper trace: N_2^+ ion current; second trace: CO^+ ion current; lower trace: light intensity registered by photomultiplier.

CONCLUSIONS

A photoionization mass spectrometer featuring a special 180 degree magnetic analyzer with inclined pole faces has been described and its usefulness as a gas analytical tool has been explored. Ion source pressures up to 20 microns have been utilized. Higher pressures can be reached but ion molecule reactions and increasing light absorption cause nonlinear ion current-pressure relationship. At 20 microns pressure, the employed spark or resonance light sources produced peak ion currents around 5×10^{-13} A. Although these ion intensities are much higher than those reported previously, they are still considerably below the ion intensities commonly produced in electron impact ion sources. It appears that comparable intensities in a photoionization mass spectrometer can be achieved if the light intensity can be increased by a factor of one thousand, but presently this can be done only at the expense of versatility by omitting the dispersing device. For this case, resonance light sources are most appropriate since they provide nearly monochromator radiation. The available intensities can be judged from measurements by Jensen and Libby [25] on a helium light source to be of the order of 10^{15} photons/cm^2 sec, or 5×10^{12} photons/sec when a slit of 5 mm high and 0.1 mm wide is used. However, only three resonance light sources are available for use in the photoionization spectral region: helium, neon, and argon. Only helium and neon sources will ionize most of the common gases. The neon light source is more favorable with respect to fragmentation than the helium source, but even the helium source produces less fragmentation than electron impact ionization. Nevertheless, several advantages of the photoionization mass spectrometer are released only in conjunction with a monochromator, including operation close to the ionization threshold and discrimination of mass doublets by the choice of appropriate ionizing energies.

ACKNOWLEDGMENTS

We have enjoyed several helpful discussions with Dr. R. F. Herzog concerning mass spectrometer problems and with Dr. J. A. R. Samson concerning vacuum ultraviolet light sources. Dr. F. F. Marmo has been a source of much encouragement and support.

This work was sponsored in part by Advanced Research Project Agency under Contract AF19(628)-3849.

REFERENCES

1. Lossing, I. P. and Tanaka, I., J. Chem. Phys. 25, 1031 (1956).

2. Herzog, R. F. and Marmo, F. F., J. Chem. Phys. 27, 1202 (1957) and in "The Threshold of Space," ed. M. Zelikoff, Pergamon Press p.124 (1957).

3. Hurzeler, H., Inghram, M. G. and Morrison, J. P., J. Chem. Phys. 27, 313 (1958); 28, 76 (1958).

4. Elder, F. A., Giese, C. F., Steiner, B. and Inghram, M. G., J. Chem. Phys. 36, 3292 (1962).

5. Steiner, B., Giese, C. F. and Inghram, M. G., J. Chem. Phys. 34, 189 (1961).

6. Weissler, G. L., Samson, J. A. R., Ogawa, M. and Cook, G. R., J. Opt. Soc. Am. 49, 338 (1959).

7. Schönheit, E., Z. Physik 149, 153 (1957).

8. Schönheit, E., Z. Naturforschung 15a, 841 (1960); 16a, 1096 (1961).

9. Comes, F. J. and Lessmann, W., Z. Naturforschung 19a, 65 (1964).

10. Comes, F. J. and Eltzer, A., Z. Naturforschung 19a, 721 (1964).

11. Schoen, R. I., J. Chem. Phys. 37, 2032 (1962).

12. Dibeler, V. H. and Reese, R. M., J. Res. Natl. Bur. Std. 68a, 409 (1964).

13. Dibeler, V. H., Reese, R. M. and Krauss, M., J. Chem. Phys. 42, 2045 (1965).

14. Dibeler, V. H., Krauss, M., Reese, R. M. and Harllee, F. N., J. Chem. Phys. 42, 3791 (1965).

15. As described by J. A. R. Samson "Vacuum Ultraviolet Light Sources," NASA CR-17, Office of Technical Services, Washington, D. C. (1963).

16. Samson, J. A. R., J. Opt. Soc. Am. 54, 6 (1964).

17. Richardson, H. O., Phys. Soc. Proc. (London) 59, 791 (1947).

18. O'Connell, J. S., Rev. Sci. Instr. 32, 1314 (1961).

19. Herzog, R. F., Z. Physik 97, 596 (1935).

20. Lampe, F. W., Franklin, J. L. and Field, F. H., in "Progress in Reaction Kinetics," Vol. I, ed. C. Porter, Pergamon Press, p.69 (1961).

21. Martin and Melton, R., J. Chem. Phys. 32, 700 (1960).

22. Field, F. H., Franklin, J. R. and Lampe, F. W., J. Am. Chem. Soc. 79, 2419 (1957).

23. Warneck, P. and Poschenrieder, W., 18th Gaseous Electronics Conference, Minneapolis, Minnesota, October (1965).

24. Dr. F. F. Marmo has pointed out that if this difficulty can be overcome, it should be possible to distinguish between many organic isomers by their ionization thresholds. For example, ortho meta and paradichlorobenzene have ionization onsets at 9.07 eV, 9.12 eV and 8.94 eV, corresponding approximately to the wavelength 1367Å, 1369Å and 1386Å which can be separated with 1Å wavelength resolution.

25. Jensen, C. A. and Libby, W. F., Phys. Rev. 135A, 1247 (1964).

26. Samson, J. A. R. and Cairns, R. B., J. Geophys. Res. 69, 4583 (1964); 70, 99 (1965).